

Critical behaviour of combinatorial search algorithms, and the unitary-propagation universality class

C. Deroulers and R. Monasson

CNRS-Laboratoire de Physique Théorique de l'ENS, 24 rue Lhomond, 75005 Paris, France.

(Dated: December 20, 2018)

The probability $P(\alpha, N)$ that search algorithms for random Satisfiability problems successfully find a solution is studied as a function of the ratio α of constraints per variable and the number N of variables. P is shown to be finite if α lies below an algorithm-dependent threshold α_A , and exponentially small in N above. The critical behaviour is universal for all algorithms based on the widely-used unitary propagation rule: $P[(1 + \epsilon)\alpha_A, N] \sim \exp(-N^{1/6} \Phi(\epsilon N^{1/3}))$. Exponents are related to the critical behaviour of random graphs, and the scaling function Φ is exactly calculated through a mapping onto a diffusion-and-death problem.

Introduction. The discovery of universality in phase transition phenomena was a major progress in modern condensed matter and statistical physics. The purpose of this letter is to point out that universality also takes place in computer science, more precisely, in computational complexity theory. There, the goal is to understand whether a computational task consisting in processing a large number N of input data can be carried out in a time scaling only polynomially *e.g.* N^3 , and not exponentially *e.g.* 2^N , with N [1]. Depending on input data defining parameters, dynamical phase transitions between these two behaviours may take place [2, 3, 4]. We prove hereafter, for the case of the celebrated Satisfiability (SAT) problem [1], that the onset of complexity at criticality is universal in that it depends on some structural features of resolution algorithms and input data statistics only.

Definitions of computational task and algorithm. In the random K-SAT problem [2], one wants to find a solution to a set of $M = \alpha N$ randomly drawn constraints (clauses) over a set of N Boolean variables x_i ($i = 1 \dots N$). Each constraint reads $z_{i_1} \vee z_{i_2} \vee \dots \vee z_{i_K}$, where \vee denotes the logical OR; z_ℓ is a variable x_{i_ℓ} or its negation \bar{x}_{i_ℓ} with equal probabilities ($= \frac{1}{2}$), and (i_1, i_2, \dots, i_K) is a K -uplet of distinct integers unbiasedly drawn from the set of the $\binom{K}{N}$ K -uplets. We now study the $K = 3$ case, the smallest value for which the problem is NP-complete [1], and $K \geq 4$ later.

Our algorithms start from *tabula rasa*, then iteratively assign variables to true (T) or false (F) according to two well-defined rules (specified below), and modify the constraints accordingly *e.g.* $\bar{x}_1 \vee \bar{x}_2 \vee x_3$ becomes $\bar{x}_1 \vee x_3$ if $x_2 = T$ [2, 5]. At the end, no constraint is left (a solution is found — success case), or a contradiction is found (one variable previously assigned to, say, T is required to be F from modified constraints — failure case). The first assignment rule, UP (for unitary propagation) [5], is common to all algorithms: if a clause with a unique variable is produced at some stage of the procedure *e.g.* \bar{x}_1 , then this variable is assigned to satisfy the clause *e.g.* $x_1 = F$. The second rule is a specific and arbitrary prescription taking over UP when it cannot be used *i.e.* in

the absence of unique variable clause. In the simplest algorithm, referred to as R (random), the prescription consists in setting any unknown variable to T or F with prob. $\frac{1}{2}$ independently of the remaining clauses [5]; more sophisticated prescriptions [6, 7] will be studied later.

Resolution procedures used in practical applications are based on the combination of the above algorithm and a backtracking principle [2]: in case of failure, the last variable assigned through the prescription (not through UP) is flipped, and the algorithm resumes from this stage. At the end, either a solution is found or all possible backtracks have failed, and a proof of the absence of solution is obtained. The resolution time typically scales as $O(N)$ if $\alpha < \alpha_A$ and $\exp O(N)$ if $\alpha > \alpha_A$, where the threshold α_A depends on the algorithm. Intuition suggests and analyses prove [4, 8] that this poly/exp crossover is due to the success/failure transition of the pure algorithm *i.e.* without backtracking. More precisely, α_A can be identified with the ratio at which the probability $P_{\text{succ}}(\alpha, N)$ of success of the pure algorithm vanishes as $N \rightarrow \infty$ [5]. To understand the onset of complexity at α_A , it is thus natural to analyze how P_{succ} vanishes when the ratio α is kept close to its critical value and N increases.

Analysis of the R algorithm. Each time a new variable is assigned some clauses are eliminated, other are reduced or left unchanged. We thus characterize the set of clauses by its state $(C_1(T), C_2(T), C_3(T))$, where C_j is the number of j -clauses *i.e.* involving j variables ($j = 1, 2, 3$) and T is the number of assigned variables [4, 5]. Consider a 3-clause left at ‘time’ T . When $T \rightarrow T + 1$, the newly assigned variable has a probability $3/(N - T)$ to appear (as is, or negated) in this 3-clause; if so the clause will be satisfied or reduced into a 2-clause (with equal prob. $\frac{1}{2}$). As a consequence the average change of C_3 equals $-3C_3(T)/(N - T)$. In the large N limit, the density $c_3(t) = C_3(tN)/N$ of 3-clauses becomes concentrated around its average value, solution of the ordinary differential equation $dc_3/dt = -3c_3/(1 - t)$. A similar reasoning leads to $dc_2/dt = 3c_3/2/(1 - t) - 2c_2/(1 - t)$ for the density c_2 of 2-clauses. Solving these equations with initial conditions $c_3(0) = \alpha$, $c_2(0) = 0$ gives $c_3(t) = \alpha(1 - t)^3$, $c_2(t) = \frac{3}{2}\alpha t(1 - t)^2$ and the resolution

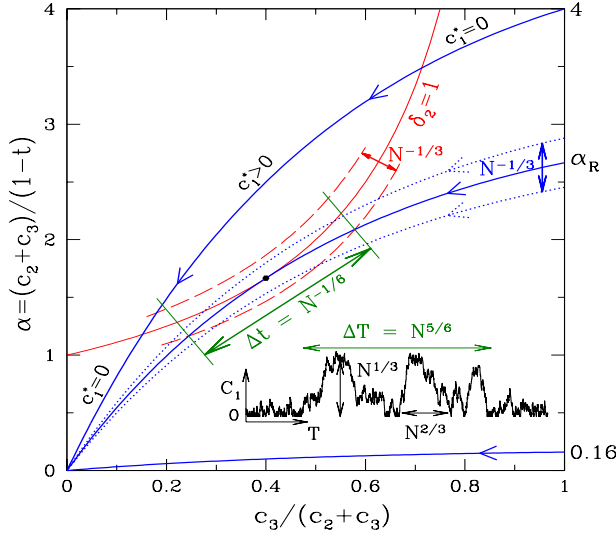


FIG. 1: Resolution trajectories for the R algorithm (bold lines, arrows indicate time direction, from a fraction $t = 0$ of eliminated variables – right axis – to $t = 1$ – lower left corner where a solution is found). For initial ratio $\alpha < \alpha_R$, C_1 keeps bounded (success case). When $\alpha > \alpha_R$, $C_1 \sim N$ when the trajectory lies above the contradiction line $\delta_2 = 1$, and the density c_1^* is positive (failure case). At the critical ratio $\alpha_R (= \frac{8}{3})$, the trajectory hits tangentially (black dot) the contradiction line. The critical region is defined by fluctuations $\sim N^{-1/3}$ for finite size N around these two lines (dotted and dashed lines respectively), and is crossed through assignment of a fraction $\Delta t = N^{-1/6}$ of variables. **Inset:** C_1 vs. T in the critical region for a particular run with $N = 10^5$ and $\alpha = \alpha_R$. Reported scalings correspond to the largest components ($S \sim N^{2/3}$).

trajectories of Fig. 1 [4].

The above evolution for c_2, c_3 is correct as long as no contradiction has emerged as a result of the production of two opposite 1-clauses *e.g.* x_1 and \bar{x}_1 . The probability $P_N(C_1; T)$ that the assignment of T variables has produced no contradiction and a set of constraints with C_1 1-clauses obeys a Markovian evolution from T to $T + 1$ with a transition matrix [4],

$$H_N[C_1' \leftarrow C_1; T, C_2] = \sum_{s_2, r_2} \mathcal{M}_{p_2}^{C_2; s_2, r_2} \left[\mathbb{I}_{C_1} \mathbb{I}_{C_1' - r_2} + (1 - \mathbb{I}_{C_1}) \sum_{s_1} \mathcal{M}_{p_1}^{C_1 - 1; s_1, 0} \mathbb{I}_{C_1' - C_1 + 1 + s_1 - r_2} \right] \quad (1)$$

where \mathbb{I}_C denotes the Kronecker function: $\mathbb{I}_C \equiv 1$ if $C = 0, 0$ otherwise. Variables appearing in (1) are as follows: s_j (respectively r_j) is the number of j -clauses which are satisfied (resp. reduced to $j - 1$ clauses) when the $(T + 1)^{th}$ variable is assigned. These are stochastic variables drawn from multinomial distributions $\mathcal{M}_p^{C; x, y} \equiv \binom{C}{x, y} p^{x+y} (1 - 2p)^{C-x-y}$. Parameter $p_j \equiv j/2/(N - T)$ equals the probability that a j -clause contains the variable just assigned; $r_1 = 0$ demands that no opposite 1-clauses and thus no contradiction are present. Equation (1) defines a random motion for a walker moving on the

semi-infinite line $C_1 \geq 0$ with time-dependent and random (through C_2) rates. The success/failure transition takes place when the average number $\delta_2 = c_2/(1 - t)$ of 1-clauses created from 2-clauses (right move) exceeds the number of 1-clauses (1 [16]) eliminated by UP each time a variable is assigned (left move) [5].

Successful regime ($\delta_2 < 1$). If elimination of 1-clauses is faster than creation, C_1 keeps bounded throughout the search process. On time scales $1 \ll T \ll N$, C_1 reaches equilibrium, with a distribution $p_0(C_1, t)$ function of slow variables only *i.e.* c_2, t . This, and the probability of success can be derived with the simple Ansatz $P_N(C_1; T) = p_0(C_1, t) + p_1(C_1, t)/N + O(N^{-2})$ and sending $N \rightarrow \infty$. We find that $p_0(C_1, t) \sim \exp(-\rho C_1)$ at large C_1 , where ρ is the time-dependent positive root of $\rho/\delta_2(t) = 1 - e^{-\rho}$. As expected, $\rho > 0$ and C_1 is bounded as long as $\delta_2 < 1$. At fixed ratio α , δ_2 reaches its maximum $\delta_2^M = \frac{3}{8}\alpha$ along the resolution trajectory for a fraction $t_R = \frac{1}{2}$ of assigned variables; the transition takes thus place at $\alpha_R = \frac{8}{3}$ [5]. The probability of success is given by $P_{\text{succ}} = \sum_{C_1} p_0(C_1, 1) = \exp[\frac{1}{2r} - \text{arctanh}(1/\sqrt{r-1})/2/\sqrt{r-1}]$ with $r = \alpha_R/\alpha$, and is shown in Fig. 2 (top inset). Note that $-\ln P_{\text{succ}}[\alpha_R(1 - \epsilon)] \sim \frac{\pi}{4} \epsilon^{-1/2}$ as α reaches its critical value α_R from below [9].

Failure regime ($\delta_2 > 1$). When $\alpha > \alpha_R$, the resolution trajectory crosses the contradiction line $\delta_2 = 1$ (Fig. 1). C_1 then becomes of the order of N and each assignment has a finite probability to produce some contradiction; the probability of success is thus exponentially small with N [10]. Later the trajectory crosses the contradiction line back and $C_1 = O(1)$ again. This behaviour is captured with the Ansatz $P_N(C_1; T) = \exp(-N\omega(c_1, t))$ where ω is the rate function associated to the large deviations of the density c_1 of 1-clauses. ω fulfills a first order partial differential equation [4, 10], which can be explicitly solved for ratios slightly above the threshold *i.e.* $\alpha = \alpha_R(1 + \epsilon)$. The coordinates c_1^*, ω^* of the minimum of ω *i.e.* the most likely trajectory are, at time $t = \frac{1}{2}(1 + s\sqrt{\epsilon})$: $c_1^* = 0, \omega^* = 0$ if $s < -1$; $c_1^* = \frac{1}{2}(1 - s^2)^2 \epsilon^2, \omega^* = [-\frac{s^5}{20} - \frac{s^3}{6} + \frac{s}{4} + \frac{2}{15}] \epsilon^{5/2}$ if $|s| < 1$; $c_1^* = 0, \omega^* = \frac{4}{15} \epsilon^{5/2}$ if $s > 1$. Thus, $-\ln P_{\text{succ}} \sim \frac{4}{15} \epsilon^{5/2} N$ to the lowest order in ϵ .

Critical regime ($\delta_2 \simeq 1$). For N large but finite and α close to α_R , finite-size scaling [2] applies if

$$-\ln P_{\text{succ}}\left((1 + \epsilon) \alpha_R, N\right) = N^\lambda \Phi(\epsilon N^\theta) \quad (2)$$

for some regular function Φ . In the infinite size N limit, this expression should agree with the above results for the successful ($\epsilon < 0$) and failure ($\epsilon > 0$) regimes. Matching the powers in N and ϵ , we find $\lambda - \frac{\theta}{2} = 0$, $\Phi(x) \sim \frac{\pi}{4} |x|^{-1/2}$ as $x \rightarrow -\infty$, and $\lambda + \frac{5\theta}{2} = 1$, $\Phi(x) \sim \frac{4}{15} x^{5/2}$ as $x \rightarrow +\infty$. As a result, $\lambda = \frac{1}{6}$ and $\theta = \frac{1}{3}$. Figure 2 (lower inset) shows the good agreement of numerical experiments performed at the critical point with the prediction $-\ln P_{\text{succ}} \sim N^{1/6}$.

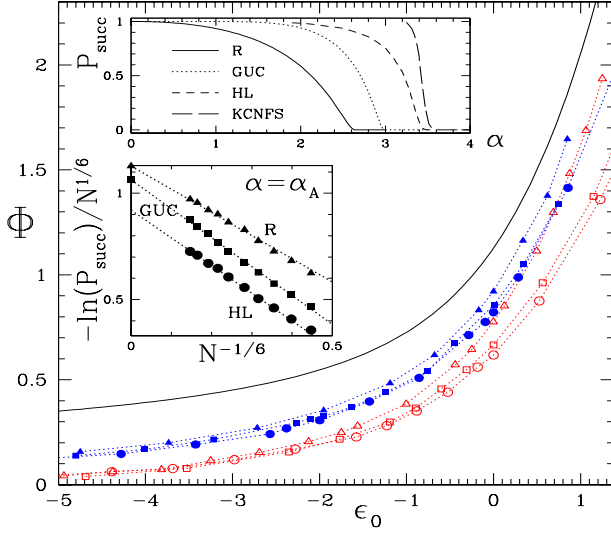


FIG. 2: Scaling function Φ (solid line) compared to numerical simulations for $N = 1000$ (empty), 20000 (filled symbols) and algorithms R (Δ), GUC (\square) and HL (\circ). Error bars (with $\simeq 10^5$ samples) are smaller than symbol size. Data for GUC and HL are rescaled horizontally and vertically, see text. Dotted lines serve as a guide for the eye. **Bottom inset:** $-\ln(P_{\text{succ}})/N^{1/6}$ vs. $N^{-1/6}$ at the critical thresholds $\alpha_R, \alpha_{\text{GUC}} \simeq 3.003, \alpha_{\text{HL}} \simeq 3.425$. Linear fits (dotted lines) extrapolate to theoretical predictions for $\Phi(0)$ (available for R and GUC) on the left axis. **Top inset:** P_{succ} vs. α showing the algorithm-dependent success/failure transition. Curves are analytical for R, GUC, and numerical for HL, KCNFS.

Introduction of the oriented graph G representing 1- and 2-clauses allows us to understand the above scalings. G is made of $2(N - T)$ vertices (one for each variable x_i and its negation \bar{x}_i), C_1 marked vertices (one for each 1-clause z_i), and $2C_2$ edges ($z_i \vee z_j$ is represented by two oriented edges $\bar{z}_i \rightarrow z_j$ and $\bar{z}_j \rightarrow z_i$) [11]. δ_2 is simply the average (outgoing) degree of vertices in G . A step of UP corresponds to removing a marked vertex (and its attached outgoing edges), after having marked its descendents; steps are repeated until the connected component is entirely removed (no vertex is marked). Then a vertex is picked up according to the prescription and marked, and UP resumes. A contradiction arises when two ‘opposite’ vertices *i.e.* associated to opposite variables are marked. The success/failure transition coincides with the percolation transition on G *i.e.* $\delta_2 = 1$ as expected. From random graph theory [11, 12], in the percolation critical window $|\delta_2 - 1| \sim N^{-1/3}$, the probability that a vertex belongs to a component of size S is $Q(S) \sim S^{-3/2}$, with a cut-off equal to the largest size, $N^{2/3}$ [13]. From Fig. 1, departure ratios α have to differ from α_R by $N^{1/3}$ for resolution trajectories to fall into the critical window. Hence $\theta = \frac{1}{3}$. The time spent by resolution trajectories in the critical window is $\Delta t \sim \sqrt{|\delta_2 - 1|} \sim N^{-1/6}$, corresponding to $\Delta T = N \Delta t \sim N^{5/6}$ eliminated variables. Let S_1, S_2, \dots, S_J be the sizes of components eliminated by UP in the crit-

ical window; we have $J \sim \Delta T / \int dS Q(S) S \sim N^{1/2}$. During the j^{th} elimination, the number of marked vertices ‘freely’ diffuses, and reaches $C_1 \sim \sqrt{S_j}$ (Inset of Fig. 1). The probability that no contradiction occurs is $[(1 - q)^{C_1}]^{S_j} \sim e^{-S_j^{3/2}/N}$ where $q \sim \frac{1}{N}$ is the probability that a marked vertex is ‘opposite’ to the one eliminated by UP. Thus $-\ln P_{\text{succ}} \sim J \int dS Q(S) S^{3/2}/N \sim N^{1/6}$, giving $\lambda = \frac{1}{6}$. Notice that, while the average component size is $S \sim N^{1/3}$ (and thus $P_N(C_1 = 0) \sim N^{-1/3}$), the value of λ is due to the largest components with $S \sim N^{2/3}$ *i.e.* $C_1 \sim N^{1/3}$ marked vertices. The distribution of $c = C_1/N^{1/3}$ is calculated below.

Scaling function. To calculate Φ in (2), we magnify the critical region in Fig. 1 and consider ratios $\alpha = \frac{8}{3}(1 + \epsilon_0 N^{-\theta})$ and times $t = \frac{1}{2}(1 + t_0 N^{-\tau})$, where θ and τ are scaling exponents to be determined. We then decompose the probability of having C_1 clauses in the critical region into the product $P_N(C_1, T) = \exp[-N^\lambda \varphi(t_0)] \times F(C_1, t_0)$; the first term is the probability that no contradiction has been found up to ‘time’ t_0 , and F is the (normalized) probability distribution of 1-clauses. Clearly $\varphi(t_0 \rightarrow -\infty) = 0$ since the probability that the search process has ended is not vanishingly small before the trajectory enters the critical region (Fig. 1). We make the Ansatz $F(C_1) = N^{-\gamma} f(c = C_1 N^{-\gamma})$ where f is the probability distribution of the rescaled number c of unit-clauses (Fig. 3). Last of all, the probability that a variable is set through a free choice and not UP, $P_N(C_1 = 0)$, is assumed to scale as f_0/N^{γ_0} .

The evolution equation for P_N based on matrix (1) imposes $\theta = \gamma = \gamma_0 = \frac{1}{3}$, $\lambda = \tau = \frac{1}{6}$ in agreement with the above scaling arguments [17]. In addition, we find $d\varphi/dt_0 = \bar{c}(t_0)$, the average value of c with distribution f solution of

$$\frac{1}{2} \frac{\partial^2 f}{\partial c^2} + v_0 \frac{\partial f}{\partial c} + (c - \bar{c}) f = 0 \quad (3)$$

with $v_0 \equiv t_0^2 - \epsilon_0$. Boundary conditions are $(\partial_c f + v_0 f)|_{c=0} = 0$ (reflecting wall) and $f_0 = f(0)/2$. The diffusion term in (3) reflects the Gaussian stochastic nature of 2- to 1-clauses reductions, the drift term favors small (respectively large) values of the density c when $v_0 > 0$ (resp. $v_0 < 0$) – corresponding to $\delta_2 < 1$ and $\delta_2 > 1$ respectively – and the third term expresses the relative death-rate of search processes with respect to the average rate \bar{c} (the higher c , the more likely it is to encounter a contradiction) [18]. The solution of differential equation (3) reads $f(c) \propto \exp(-v_0 c) \text{Ai}[\sqrt[3]{2}c + z(v_0)]$, where Ai is the Airy function, $z(x)$ is the inverse function of $x(z) = -\sqrt[3]{2} \text{Ai}'(z)/\text{Ai}(z)$. Distribution f is shown on Fig. 3 for several values of the drift. Positive (respectively negative) v_0 correspond to trajectories below (resp. above) the contradiction line (Fig. 1), with distributions f peaked around $c = 0$ (resp. $c > 0$).

The probability of success remains unchanged (to the leading order in N) once the trajectory exits from the

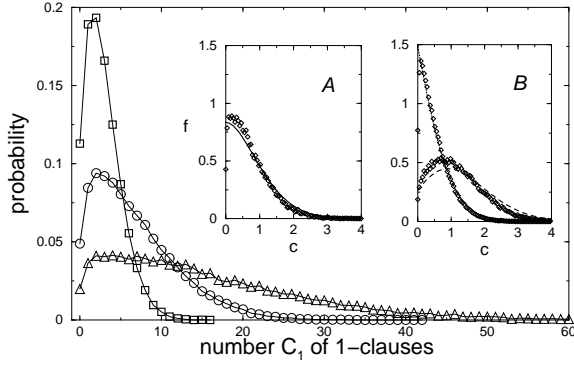


FIG. 3: Histograms of the numbers C_1 of 1-clauses for sizes $N = 10^2$ (\square), 10^3 (\circ) and 10^4 (\triangle) right at criticality (time $t = \frac{1}{2}$ and ratio $\alpha = \frac{8}{3}$). Note the sharp increase of the probability around $C_1 = 0$, in quantitative agreement with the theoretical prediction $f_0 = f(0)/2$. **Insets:** theoretical distributions f for $c = C_1/N^{1/3}$ at criticality (A, same data as main figure), and for drifts $v_0 = 0.5$ (B, dotted), $v_0 = -0.7$ (B, dashed curve) compared to numerics.

critical region, thus $-\ln P_{\text{succ}}/N^\lambda = \varphi(t_0 \rightarrow +\infty)$. This proves the existence of the scaling function defined in (2), with

$$\Phi(\epsilon_0) = \frac{1}{4} \int_{-\epsilon_0}^{+\infty} \frac{dx}{\sqrt{\epsilon_0 + x}} [x^2 - 2^{2/3} z(x)] \quad (4)$$

Scaling function Φ is plotted and compared to numerics in Fig. 2. It is an easy check that all the results related to the successful and failure regimes *e.g.* the values c^*, ω^* listed above for finite ϵ and $N \rightarrow \infty$ are found back when $\epsilon_0 \rightarrow \pm\infty$ respectively.

Universality. The critical point of R, or any algorithm A that implements UP *e.g.* GUC [5] or HL [6] where variables are chosen to satisfy 2-clauses or according to their occurrences respectively, is reached when the resolution trajectory is, for some time t_A , tangent to the $\delta_2 = 1$ line: $\delta_2(t_A + \Delta t) - 1 = b(\Delta t)^n$ with $n \geq 2$ even integer and b determined from the derivatives of the density c_2 of 2-clauses at t_A . The tangency condition reflects that the creation of new edges in G , from the reduction of 3- into 2-clauses, precisely compensates the elimination of edges by UP. Although the resolution trajectory strongly depends on A, the critical behaviour depends on n, b only, and is thus universal.

The value of n is 2 for R, GUC, HL and generic algorithms A. Therefore, $\theta = \frac{1}{6}, \lambda = \frac{1}{3}$ independently of A; the scaling function is $\Phi_A(\epsilon_0) = r_A^\Phi \Phi(r_A^\epsilon \epsilon_0)$ where the r_A 's are functions of b *e.g.* $r_{\text{GUC}}^\Phi \simeq 0.9423, r_{\text{GUC}}^\epsilon \simeq 0.5706$. Fig. 2 illustrates that GUC and HL fall in this UP universality class. Numerical investigations suggest that more complex algorithms as KCNFS [7] do, too. This universality class is robust against any change, either induced by algorithms or present in the input data distribution, in the degree sequence of the clauses graph G , a consequence of the robustness of the critical component size distribution $Q(S)$ [13].

Higher values of $n(\geq 4)$ are exceptionally found for finely-tuned input data statistics *e.g.* with clauses of different lengths $\ell(\leq K)$ and appropriate ratios α_ℓ (so far we have restricted to $K = 3$ with $\alpha_3 \equiv \alpha$). If the ratios at the critical point $\delta_2 = 1$ are such that the reduction of $(\ell + 1)$ - to ℓ -clauses compensates the disappearance of ℓ -clauses for all $2 \leq \ell < K$, then the resolution trajectory will stay longer in the critical region, making P_{succ} decrease. The precise condition is $\alpha_\ell = 2^{\ell-1}/\ell/(\ell-1)$ at criticality [14], leading to $\lambda = \frac{n-1}{3n}$ with $n = K-1$ [17].

It would be interesting to extend our study to structured input data distributions *e.g.* leading to clause graphs G embedded in finite-dimensional spaces, and possibly to $\theta \neq \frac{1}{3}$. In this context, developing renormalization tools to capture the critical behaviour of algorithms would be the natural yet apparently difficult next step. It would also be worth to study universality for other types of algorithms *e.g.* local search procedures [15], or other computational tasks [3] *e.g.* graph coloring [9], where poly/exp transitions take place.

-
- [1] C. Papadimitriou, K. Steiglitz, *Combinatorial Optimization*, Dover (1998).
 - [2] S. Kirkpatrick, B. Selman, *Science* **264**, 1297 (1994); B. Selman, S. Kirkpatrick, *Artificial Intell.* **81**, 273 (1996).
 - [3] S. Mertens, *Phys. Rev. Lett.* **81**, 4281 (1998); A.K. Hartmann, M. Weigt, *Phys. Rev. Lett.* **86**, 1658 (2001); A. Montanari, R. Zecchina, *Phys. Rev. Lett.* **88**, 178701 (2002); R. Mulet *et al*, *Phys. Rev. Lett.* **89**, 268701 (2002).
 - [4] S. Cocco, L. Ein-Dor, R. Monasson. in *New optimization algorithms in physics*, A. Hartmann, H. Rieger (eds), Wiley (2004) (see <http://www.lpt.ens.fr/~monasson>)
 - [5] M.T. Chao, J. Franco. *Inform. Sci.* **51**, 289 (1990); A. Frieze, S. Suen. *J. of Algorithms* **20**, 312 (1996).
 - [6] A.C. Kaporis, L.M. Kirousis, E.G. Lalas. *ESA 02, Lecture Notes in Comp. Sci.* **2461**, 574 (2002).
 - [7] G. Dequen, O. Dubois. *Proc. SAT'03*, 486 (2003).
 - [8] D. Achlioptas, P. Beame, M. Molloy, *J. Comp. Sci. Syst.* **68**, 238 (2004).
 - [9] H. Jia, C. Moore. *preprint* (2003).
 - [10] S. Cocco, R. Monasson. *Phys. Rev. E* **66**, 037101 (2002).
 - [11] B. Bollobas *et al*. *Rand. Struct. Algor.* **18**, 201 (2001).
 - [12] S. Janson, T. Luczak, A. Rucinski. *Random Graphs*, Wiley (2000).
 - [13] M.E.J. Newman, S.H. Strogatz, D.J. Watts, *Phys. Rev. E* **64**, 026118 (2001).
 - [14] C. Goldschmidt, preprint math.PR/0401208 (2004); our graph G is oriented, hence the power of 2.
 - [15] G. Semerjian, R. Monasson, *Phys. Rev. E* **67**, 066103 (2003); W. Barthel, A.K. Hartmann, M. Weigt, *Phys. Rev. E* **67**, 066104 (2003); S. Seitz, P. Orponen, *Elec. Notes Discr. Math.* **16** (2003).
 - [16] More than one clause can be satisfied especially when $C_1 \sim N$ *i.e.* in the failure regime.
 - [17] These results are not affected by the presence of Gaussian fluctuations $\sim N^{-1/2}$ in $c_2(t)$.
 - [18] Notice that (3) lacks any time derivative since f reaches stationarity on a much shorter time-scale ($N^{-1/3}$) than the one relevant for P_{succ} ($N^{-1/6}$).